Exciton luminescence kinetics in silicon under the conditions of injection of a phonon pulse

N. N. Zinov'ev, D. I. Kovalev, V. I. Kozub, and I. D. Yaroshetskiĭ

A. F. Ioffe Physicotechnical Institute, Russian Academy of Sciences, 194021 St. Petersburg, Russia
(Submitted 13 April 1994)
Zh. Eksp. Teor. Fiz. **106**, 585–595 (August 1994)

The temporal kinetics of the electronic subsystem (including free electrons and multiexciton impurity complexes) were investigated under the conditions such that free excitons are entrained by nonequilibrium acoustic phonons when the latter act on the exciton luminescence of bulk samples of pure silicon. It is shown that the trapping of free excitons on shallow impurity centers determines the relaxation of the nonequilibrium concentration of free excitons. The kinetics of free excitons under the conditions of strong and weak drag are analyzed, and the velocity of exciton drag by phonons in silicon is determined. The spatial and temporal evolution of the exciton cloud under the action of a stream of nonequilibrium acoustic phonons is described theoretically. The results are in good agreement with the experimental data.

1. INTRODUCTION

The interaction of charge carriers and phonons gives rise to a number of physical phenomena which have been studied in many investigations. The transfer of momentum from the phonons to the electronic system results in the appearance of drift in a system of free charge carriers and excitons. This phenomenon is known as drag and has been investigated in direct- and indirect-gap semiconductors.[1–4] For bound electron-hole states an effect of a different kind can be important: In this effect the energy of the absorbed phonons is sufficient for excitation or ionization of $e-h$ complexes. Exciton transport induced by nonequilibrium acoustic phonons changes the spatial distribution of photoexcited electron-hole pairs and could give rise to a number of new patterns in the luminescence kinetics. The objective of the present work is to investigate these patterns. In silicon nonequilibrium acoustic phonons with sufficiently high energies, including energies lying in the dissociation band of multiexciton impurity complexes (MEICs), propagate ballistically. This makes it possible to analyze the kinetics of electronic excitations by investigating the response of the electronic system (excitonic luminescence) to the action of a stream of nonequilibrium acoustic phonons.

In Sec. 1 we discuss the results of an investigation of the time dependence of the changes induced in the exciton luminescence by a stream of nonequilibrium acoustic phonons. In Sec. 2 data on the action of a stream of nonequilibrium acoustic phonons on the spatial distributions of electronic excitations (free excitons, MEICs) are analyzed.

2. EXPERIMENTAL PROCEDURE

We investigated p-type silicon crystals with boron concentration $N_B = 10^{13} - 10^{14}$ cm^{-3}. The crystals were parallelepipeds with the dimensions $5 \times 5 \times 15$ and $2 \times 5 \times 10$ mm^3 (Fig. 1, inset). The crystal axis is also the [110] crystallographic axis—the direction of focusing of longitudinal (L) and slow transverse (ST) phonons—or the [100] axis—the direction of focusing of fast transverse phonons.[6] A constantan film with dimensions $\sim 10 \times 1$ mm^2 and thickness ~ 300

Å, playing the role of a "heat generator," was deposited on one of the crystal faces. The film was heated by a current pulse with duration $t_0 = 0.1 - 5$ μs, maximum power of 5×10^4 W/cm^2, and a repetition frequency of 10 kHz. A helium-neon or Ar* laser was used for stationary excitation of nonequilibrium electron-hole pairs (NEHPs). The laser radiation was focused into a spot of diameter ~ 20 μm with maximum pumping density ~ 1 W/cm^2, which is below the condensation threshold of electron-hole drops. The temperature of the liquid-helium thermostat with the sample was $T \approx 1.5$ K. Spectral measurements were performed with a DFS-24 double monochromator with linear dispersion $D \sim 8$ Å/mm at wavelengths $\lambda \sim 1$ μm. The luminescence signal was recorded with a gated photon-counting system and a microcomputer was used for on-line processing of the data.

The experimental apparatus functioned in three modes.

1. Determination of the spectral dependence. The recorded luminescence signal was gated with 0.1–1 μsec pulse immediately prior to the heat pulse (spectrum in the absence of phonons) and with a similar pulse delayed with respect to the heat pulse by the ballistic transit time from the "heat generator" to the point of optical excitation (spectrum in the presence of phonons) and the differential luminescence spectrum (obtained by subtracting these two spectra) owing to the changes produced in the luminescence spectrum by the nonequilibrium acoustic phonons was recorded.[8,9]

2. Analysis of the time dependence of the corresponding luminescence lines under conditions such that electron-hole excitations interact with the nonequilibrium-acoustic-phonon pulse injected into the sample.

3. Measurement of the spatial luminescence profile. The condensing system, controlled by micrometric motors with an ORIEL 18011 Encoder Mike controller, allowed the image of the entrance slit of the monochromator to be scanned over the surface of the crystal in a 3-mm range with respect to the central position with a resolution of 20–30 μm.

The generated nonequilibrium electron-hole pairs (excitons, MEICs) become distributed over the interior of the sample to a depth on the order of the diffusion spreading of the free excitons. The stream of nonequilibrium acoustic
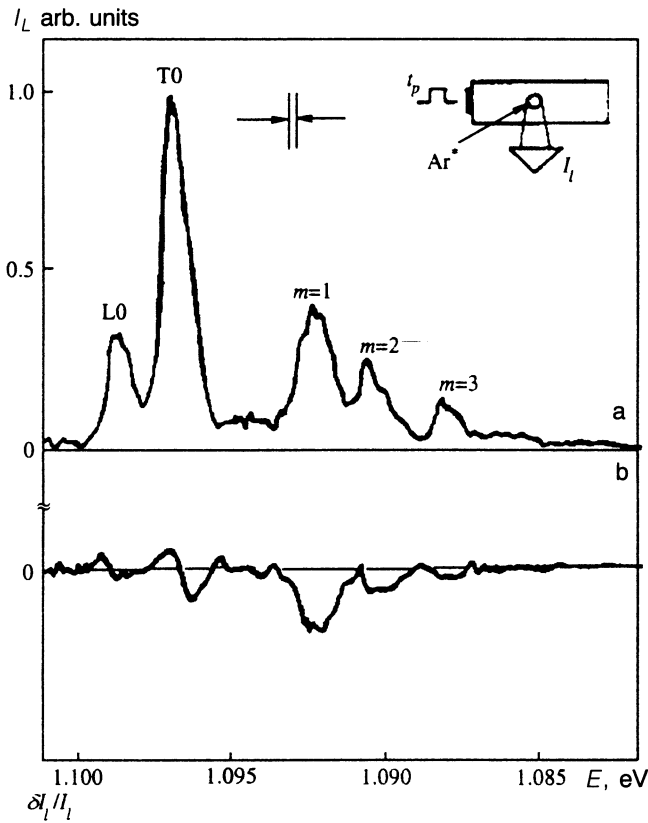
FIG. 1. (a) Luminescence spectrum of Si:B in the absence of nonequilibrium acoustic phonons and (b) differential luminescence spectrum. $T=1.4$ K, $t_0=1$ μs, $\Delta t=1$ μs, and $W=5\cdot10^{-4}$ J/mm^2.
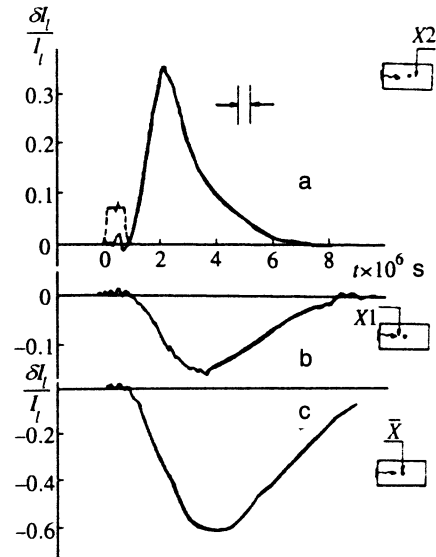

FIG. 2. Differential kinetics of free excitons at $T=1.4$ K. a—at the point $X_2=\bar{X}+\Delta X$; b—at the point $X_1=\bar{X}-\Delta X$; c—bound excitons. $W=5\cdot10^{-4}$ J/mm^2, $t_0=1$ μs, $\bar{X}=2$ mm, $\Delta X=100$ μm. The dashed curve represents the current pulse exciting the heat generator.

phonons injected into the sample during the pulsed heating of the metal film changes the initial stationary NEHP distribution, whose characteristics were investigated in the experiment (Fig. 1, inset). The geometry chosen for the experiment prevented phonon transmission through the sample/liquid-helium interface from affecting the experimental results.[4]

Figures 1a and b display the exciton luminescence spectrum of Si:B in the absence of nonequilibrium phonons and the differential luminescence spectrum. These spectra were recorded under the conditions of uniform stationary optical excitation of the crystal surface. The luminescence spectrum recorded during the gated pulse immediately prior to phonon injection (Fig. 1a) exhibits clearly LO/TO replicas of the recombination lines of free excitons and MEICs with $m=1$, 2, and 3. The differential luminescence spectrum presented in Fig. 1b reflects the result of the interaction of the injected phonons with recombinations centers (free excitons and MEICs). It is evident that the free-exciton line in the differential spectrum is characterized by an increase in the luminescence intensity on the high-energy wing and a decrease of the signal at low energies. Since the shape of the luminescence line of LO/TO replicas of free exciton lines is determined by the energy distribution function of the excitons in the band, the observed "dipolar" behavior of the differential signal reflects the simple fact that the exciton gas is heated due to the absorption of acoustic phonons with energy $\hbar\omega=E(\mathbf{k}_f)-E(\mathbf{k}_i)$. This process results in "depletion" of the exciton distribu-

tion function at low energies and hence the appearance of hot excitons. The fact that the total intensity of free-exciton emission in the differential spectrum is zero proves that the total free-exciton concentration does not change when phonons are injected with the characteristic spectrum of the "heat" generator. We now discuss the experimental data on the transport kinetics and the relaxation of electronic excitations under the experimental conditions.

A. TIME DEPENDENCE OF THE LUMINESCENCE OF FREE AND BOUND EXCITONS

The data displayed in Fig. 2c reflect the time dependence of the change induced in the intensity of the luminescence line of MEICs with $m=1$ by the phonon pulse. This measurement was performed with uniform optical excitation of the entire surface of the sample. Under these conditions $\partial n/\partial x=0$, where x is the coordinate in the plane of the excited surface of the sample, and for this reason the spatial transport of nonequilibrium electron-hole pairs does not affect the luminescence spectrum. The temporal evolution of the luminescence reflects the kinetics of the phonon distribution function at the characteristic energy at a given point in the sample. Such luminescence is essentially a phonon detector, whose response time is determined by the relaxation times in the electron-hole system and whose spatial resolution is determined by the size of the detection region (~30 μm in our case).

We now consider the temporal kinetics recorded on the TO component of the free-exciton emission and characterizing the time dependence of the electronic density caused by the arrival of the heat pulse (transport of free excitons) at the point a $\bar{X}+\Delta X$ and $\bar{X}-\Delta X$ (Figs. 2a and b), where $\bar{X}$ is the distance from the phonon generator up to the excitation point and ΔX is the distance between the point of optical genera-
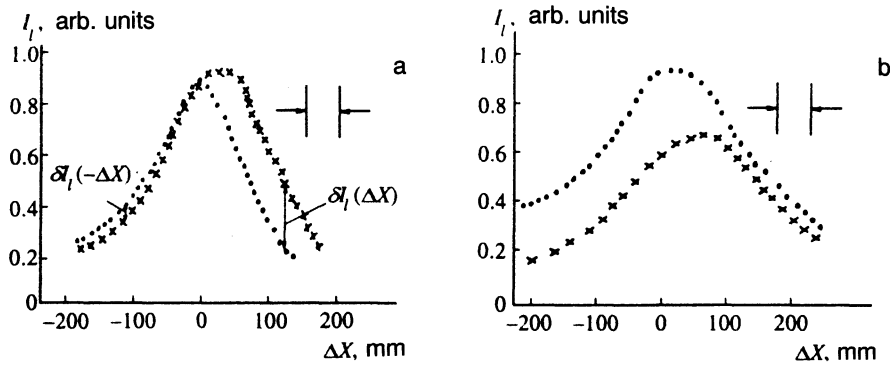
FIG. 3. Spatial distribution of free (a) and bound (b) excitons in the presence (×) and absence (●) of acoustic phonons. $T=4.2$ K, $t_0=1$ μs, $\Delta t=1$ μs, $W=5\cdot10^{-4}$ J/mm^2.

tion of the excitons and the region of signal detection, chosen so that $\Delta X \gtrsim L_d$ is the diffusion length of the excitons ($L_d \sim 100$ μsec at $T=1.5$ K) - Fig. 3a. Two main features are clearly seen: a positive signal at the point $X_2=\bar{X}+\Delta X$ and a negative signal at the point $X_1=\bar{X}-\Delta X$. The signal intensity is considerably lower at the point X_1 than at the point X_2. A difference is also observed in the slopes of the leading edge of the recorded time dependence and in the times at which the maximum amplitudes of the kinetics is reached.

Two factors could be responsible for the appearance of the phonon-induced signal on the exciton line: exciton transport, as a result of exciton drag by nonequilibrium acoustic phonons, into the region of the crystal whence luminescence is detected; and ionization of the bound states of MEICs by nonequilibrium phonons. In the first case, in the experimental geometry considered, the signal should increase near $\bar{X}+\Delta X$ and correspondingly decrease near $\bar{X}-\Delta X$. In the second case—ionization of MEICs by phonons— the exciton luminescence intensity should increase near both $\bar{X}+\Delta X$ and $\bar{X}-\Delta X$. We ignore the ionization of free excitons, since under the experimental conditions the nonequilibrium acoustic phonons with energies $\hbar\omega_{ph}>R_{ex}$ are not generated (R_{ex} is the excitonic Rydberg; in Si $R_{ex}=14.5$ meV[9]). As far as the durations of the leading and trailing edges of the pulse in the time-of-flight spectrum are concerned, it is obvious that they must be determined by the drift and diffusion velocities, respectively, of the free excitons, the probabilities of ionization of MEIC, and the binding of excitons in states of MEICs. It can be inferred that all these factors determine the experimental curves. We discuss first the possibility of ionization of MEICs by a stream of nonequilibrium acoustic phonons. To exclude effects associated with free-exciton transport the spectra were studied under the conditions of uniform optical excitation. As one can see from Fig. 1b, decreasing the intensity of the MEIC luminescence lines does not increase the signal on the free-exciton emission line. The decrease MEIC luminescence intensity as a result of absorption of acoustic phonons could be caused by two processes: ionization of the bound state by phonons and transfer of the complex into a state with an efficient nonradiative decay channel. The experiment (Fig. 1) indicates that ionization according to the scheme (MEIC)$_m$ + $\hbar\omega_q\rightarrow$(MEIC)$_{m-1}$ + free exciton (ionization of a MEIC with detachment of an exciton as a whole) does not play a significant role in energy exchange processes

MEICs$\leftrightarrow$ acoustic phonons. Indeed, the probability $W(\mathbf{q})$ of excitation of a bound state by acoustic phonons with momentum $\mathbf{q}$ is determined by the Fourier component of the wave function of the bound exciton in the momentum representation $W(\mathbf{q})$:

$$W(\mathbf{q})=|F(\mathbf{q})|^2\propto\frac{1}{[q^2+(1/a^*)^2]^4},\qquad(1)$$

where $a=\sqrt{(\hbar^2/2m^*\Delta\epsilon)}$, $q=\Delta\epsilon/\hbar s$, $\Delta\epsilon$ is the MEIC binding energy, and s is the sound speed. Substituting the values $\Delta\epsilon=4$ meV and $s=10^6$ cm/sec we obtain $(qa^*)\sim10$, which lowers the probability of interaction of acoustic phonons with MEICs considerably. This circumstance could be why free excitons do not appear as a result of the change produced in the number of MEICs by nonequilibrium acoustic phonons (Fig. 1b). A different mechanism for ionization of bound excitons is the scheme (MEIC)$_m$ + $\hbar\omega_q$ $\rightarrow$(MEIC)$^*_{m-1}$ + e. In this situation a free carrier e appears and the complex (MEIC)$_m$ is transferred into the charged state (MEIC)$^*_{m-1}$, determined by the sign of e. Such centers of the hydrogen-ion type (H^+,H^-) are well known as D^- and A^+ centers, and they have been observed, in particular, in experiments on IR photoconductivity[10,11] as well as in experiments with nonequilibrium phonons.[12] As far as the binding energy of the carrier e is concerned, it will be significantly lower than the binding energy of MEICs, and in silicon $\Delta\epsilon\sim1$–2 meV. In this model of dissociation the form factor $|F(\mathbf{q})|^2$ is 10^2–10^4 times larger than in the case of dissociation of MEICs with detachment of an $e-h$ pair as a whole. Thus the form of the time dependence of the luminescence signal can be determined by the phonon kinetics in the crystal (determining the exciton drag process) and the relaxation of the nonequilibrium spatial distribution of excitons by means of binding/dissociation and diffusion processes.

The scattering of nonequilibrium acoustic phonons by free excitons results in heating of the exciton gas and directed motion of the exciton cloud—the drag effect (low-frequency phonons with energies $\hbar\omega_q<2$ meV, which in pure silicon propagate ballistically, make the main contribution to scattering of phonons by excitons). The entrainment of free excitons by nonequilibrium phonons was studied at different phonon-stream intensities: The energy of the pulse on the
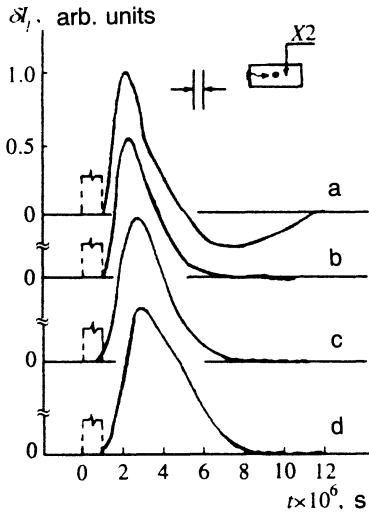
FIG. 4. Differential kinetics of free excitons as a function of the energy of the heat pulse at $T=4.2$ K; a—$W=5\cdot10^{-3}$ J/mm^2, b—$W=5\cdot10^{-4}$ J/mm^2, c—$W=10^{-4}$ J/mm^2, d—$W=2\cdot10^{-5}$ J/mm^2; the pulse duration $t_0=1$ μs =const.

heat generator was varied by increasing the pulse duration while maintaining a constant amplitude and by increasing the amplitude of the pulse while maintaining a constant pulse duration. According to Fig. 4 the temporal kinetics at the point $\bar{X}+\Delta X$ does not change much as the energy of the heat pulse increases. As the energy of the heat pulse increases, the half-width of the temporal kinetics and the time interval between the heat pulse and the signal maximum decrease. In addition, the sign of the signal at maximum energies (10^{-3} J/mm^2) changes. Significant asymmetry of the kinetics for the regions $\bar{X}+\Delta X$ and $\bar{X}-\Delta X$ occurs for all energies except at the lowest values ($5\cdot10^{-5}$ J/mm^2), when the kinetics are practically symmetric. It should be underscored that the character of the signal does not depend on the quality of the surface treatment of the sample. This shows that phonons propagating along the axis of the sample make the main contribution to the observed signal (the mean free path of acoustic phonons in Si can reach, according to Refs. 5–7, ~1–2 cm under our conditions).

B. SPATIAL DISTRIBUTION OF FREE AND BOUND EXCITONS UNDER THE ACTION OF A STREAM OF NONEQUILIBRIUM PHONONS

A direct consequence of the drag of free excitons is that the spatial distribution of excitonic luminescence changes as a result of the action of the directed flux of acoustic phonons. We recorded simultaneously the spatial distribution of the excitons in both the absence and presence of a phonon stream (Fig. 3a). It is obvious that the stationary distribution is displaced in the direction of propagation of the phonons with the total number of excitons being conserved. The observed displacement $\Delta X=50$ μm over a time ~1 μsec with respect to the end of the heat pulse (this time corresponds to the signal maximum in Fig. 2a makes it possible to determine the exciton drag velocity: $v_d=5\cdot10^3$ cm/sec. The "dis-

placement" of the spatial distribution of bound excitons, which corresponds to changes in the distribution of the free excitons (Fig. 3b), confirms that the exciton trapping on impurity centers is effective for the relaxation of the excess free-exciton concentration. Consequently, the process of trapping of excitons on impurity centers should play a considerable role in the formation of the phonon-induced temporal kinetics of exciton luminescence.

To describe the spatial and temporal evolution of the exciton cloud under the action of a stream of nonequilibrium acoustic phonons we employ the diffusion equation with drift in which the action of the phonons on the excitons is taken into account by introducing the drift velocity v_d (see, for example, Ref. 1):

$$\frac{\partial n}{\partial t} - D\frac{\partial^2 n}{\partial x^2} + v_d\frac{\partial n}{\partial x} + \frac{n}{\tau} = I\delta(x). \quad (2)$$

Here n is the exciton concentration and τ is the exciton lifetime (with respect to trapping on centers). The right-hand side describes the source of excitons: I is the intensity of the source, and the dimensions of the source are assumed to be smaller than the characteristic spatial scale ΔX of the problem. In turn, the smallness of ΔX compared to the distance to the phonon source makes it possible to regard the problem as one-dimensional.

The change, of interest to us, in the luminescence signal (determined by the change in the local exciton concentration n) is evidently connected with the time dependence of the drift velocity v_d. For simplicity we consider a square phonon pulse: $v=v_0\Theta(t)$. For $t<0$ (i.e., in the absence of a phonon pulse) $v_d=0$ and we have from the expression (2)

$$n=\varphi(x)\equiv\frac{1}{2}I\sqrt{\frac{\tau}{D}}\exp\left(-\frac{|x|}{\sqrt{D\tau}}\right). \quad (3)$$

For the region $t>0$ ($v_d=0$) the solution (3) is used as an initial condition. The general solution of Eq. (2) has the form

$$n=\exp\left(-\frac{t}{\tau}\right)\int_{-\infty}^{+\infty}\varphi(\xi')\frac{\exp\left(-\dfrac{(x-v_dt-\xi')^2}{4Dt}\right)}{\sqrt{2\pi Dt}}d\xi'$$

$$+I\int_0^t\exp\left(-\frac{t'}{\tau}\right)\frac{\exp\left(-\dfrac{(x-v_dt')^2}{4Dt}\right)}{\sqrt{2\pi Dt'}}dt'. \quad (4)$$

Analyzing the expression (4) we can separate two limiting cases:

a) $v_d^2\ll D/\tau$—weak drag. In this case, expanding Eq. (4) up to first order in v_d, we have

$$\delta n=n-n(t<0)$$

$$=\exp\left(-\frac{t}{\tau}\right)v_d\int_{-\infty}^{+\infty}\varphi(\xi')\frac{(x-\xi')}{2D\sqrt{2\pi Dt}}$$

$$\times\exp\left(-\frac{(x-\xi')^2}{4Dt}\right)d\xi'$$

$$+ I v_d \int_0^t x \, \exp\left(-\frac{t'}{\tau}\right) \frac{\exp\left(-\dfrac{x}{4Dt'}\right)}{4D\sqrt{2\pi Dt'}} \, dt'. \tag{5}$$

We call attention of the fact that the first term is odd as a function of x, since it changes sign under the substitutions $x \Rightarrow -x$ and $\xi' \Rightarrow -\xi'$, and since the second term is also odd as a function of x, it follows that in the case of weak drag the differential signal δn is odd as a function of x and has the same time dependence for $x>0$ and $x<0$, in agreement with the experiment with heat-pulse energy densities $\approx 10^{-5}$ J/mm^2.

b) $v_d^2 \gg D/\tau$—strong drag. In this situation analysis of the expression (4) gives the following estimate:

$$\delta n \approx I \sqrt{\frac{\tau}{D}} \left\{ \exp\left(-\frac{|x|}{\sqrt{Dt}}\right) \left[\exp\left(-\frac{|x-v_d t|-|x|}{\sqrt{Dt}} - \frac{t}{\tau}\right) - 1\right] \right.$$
$$\left. + \frac{\sqrt{Dt}}{\tau v_d} \Theta(v_d t - x) \right\}. \tag{6}$$

In the case $x<0$

$$\delta n \approx I \sqrt{\frac{\tau}{D}} \left\{ \exp\left(\frac{x}{\sqrt{Dt}}\right) \left[\exp\left(-\frac{v_d t}{\sqrt{Dt}} - \frac{t}{\tau}\right) - 1\right] \right\}. \tag{7}$$

At $t=0$ (phonon pulse is switched on) we have $\delta n=0$; δn decreases with increasing t and for $t > \sqrt{(D\tau/v_d^2)}$ reaches the value $\delta n(x,t)/n(x,t=0) \sim -1$, after which it remains constant over the time of action of the phonon pulse.

For the region $x>0$ two time intervals can be distinguished. For $t<x/v_d$

$$\delta n \approx n(x=0,t=0)\left\{ \exp\left(-\frac{x}{\sqrt{Dt}}\right) \left[\exp\left(\frac{v_d t}{\sqrt{Dt}} - \frac{t}{\tau}\right) - 1\right] \right\}. \tag{8}$$

It is evident that the signal increases with t, reaching a maximum at $t=x/v_d$, and $\delta n_{max} \sim n(x=0,t=0)$. This is the result of a "displacement" of the initial exciton cloud.

For $t>x/v_d$ we have

$$\delta n \approx n(x=0,t=0)\left\{ \exp\left(-\frac{x}{\sqrt{Dt}}\right) \right.$$
$$\left. \times \left[\exp\left(-\frac{v_d t + 2x}{\sqrt{Dt}} - \frac{t}{\tau}\right) - 1\right] + \sqrt{\frac{D}{\tau}} \frac{1}{v_d} \right\}. \tag{9}$$

In this case δn decreases with increasing t up to values

$$\delta n \approx n(x=0,t=0)\left[\sqrt{\frac{D}{\tau}} \frac{1}{v_d} - \exp\left(-\frac{x}{\sqrt{D\tau}}\right)\right] \tag{10}$$

so that for $x<\sqrt{D\tau}$, $\delta n|_{t\to\infty}<0$, and $\delta n \sim n(x,t=0)$. The increment δn vanishes at $t \sim (\sqrt{D\tau/v_d}) + 2x/v_d$. It is easy to see that these expressions describe qualitatively the experimentally observed time dependence (in particular, the change in the sign of δn for $\Delta X>0$ in the case of strong phonon pulses—Fig. 4a).

Analyzing the time interval corresponding to the end of the phonon pulse, we can use as the initial condition at the time $t=t_0$ the distribution
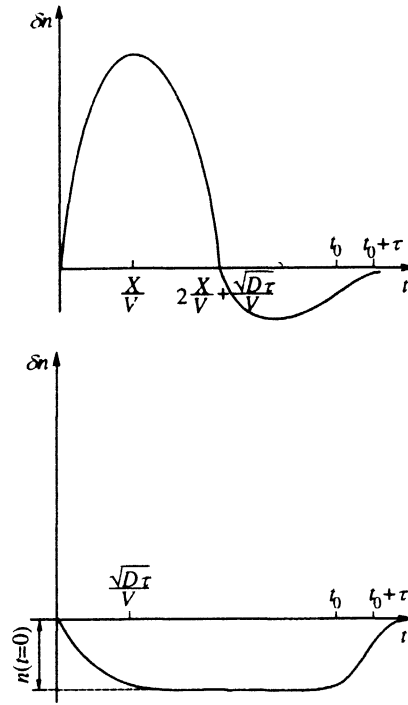

FIG. 5. Differential kinetics of a free exciton in the case of strong drag: a—response in the region $X>0$, b—response in the region $X<0$.

$$n(x<0)=0; n(x>0) \approx \frac{I}{v_d} \exp\left(-\frac{x}{v_d \tau}\right) \tag{11}$$

or, measuring time from $t=t_0$ $(t \to t - t_0)$

$$n = \exp\left(-\frac{t}{\tau}\frac{I}{v_d}\right) \int_0^{v_d t} \frac{\exp\left(-\dfrac{(\xi-\xi')^2}{4Dt}\right)}{\sqrt{2\pi Dt}} \, d\xi'$$
$$+ I \int_0^t \frac{\exp\left(-\dfrac{t'}{\tau} - \dfrac{x^{2'}}{4Dt'}\right)}{\sqrt{2\pi Dt'}} \, dt'. \tag{12}$$

For x not exceeding $\sqrt{D\tau}$ significantly, the first term can be neglected, and the second term describes the restoration of the initial exciton distribution over a time $t-t_0 \sim \tau$. Thus the following conclusions can be drawn from the analysis presented above. For weak phonon pulses the signals for the regions $\Delta X>0$ and $\Delta X<0$ are symmetric; this agrees with experiment. In the limit of high intensities the signals are strongly asymmetric; the schematic form of the signals is displayed in Fig. 5. As one can see from the data presented, for the region $x<0$ in the strong-drift regime the theory predicts that the signal increases more rapidly (over a time $\sim \sqrt{D\tau/v_d}$) than it decays (over a time τ), since in this regime $v_d^2 \gg D/\tau$. The behavior of the signal in the region

$$\sqrt{D\tau} \ll t < t_0 \quad \text{for } x<0$$

and

$$(2x/v_d) + \sqrt{D\tau}/v_d \ll t < t_0 \quad \text{for } x>0,$$

is evidently determined by the shape of the phonon pulse (in our model the pulse is square). An estimate for v_d from Eq. (8) based on the data on time-of-flight spectra gives $v_d = 5 \cdot 10^3$ cm/sec, which agrees with the estimate obtained by analyzing the spatial distributions of the excitons. Thus comparing the experimental curves to the predictions of the model shows that the observed effects can be described on the basis of the idea of drift of free excitons under the action of the phonon pulse.

[1] V. S. Bagaev, L. V. Keldysh, N. N. Sibel'din, and V. A. Tsvetkov, Zh. Eksp. Teor. Fiz. **70**, 702 (1976) [Sov. Phys. JETP **43**, 362 (1976)].

[2] N. N. Zinov'ev, U. Parmanbekov, and I. D. Yaroshetskiĭ, Pis'ma Zh. Eksp. Teor. Fiz. **33**, 601 (1981) [JETP Lett. **33**, 584 (1981)].

[3] N. N. Zinov'ev, L. P. Ivanov, V. I. Kozub, and I. D. Yaroshetskiĭ, Zh. Eksp. Teor. Fiz. **84**, 1761 (1983) [Sov. Phys. JETP **57**, 1027 (1983)].

[4] A. V. Akimov, A. A. Kaplyanskiĭ, and E. S. Moskalenko, and R. A. Titov, Zh. Eksp. Teor. Fiz. **94**, 307 (1988) [Sov. Phys. JETP **67**, 2348 (1988)].

[5] D. Marx and W. Eisenmenger, Z. Phys. B **48**, 277 (1982).

[6] D. C. Hurley and J. P. Wolfe, Phys. Rev. B **32**, 2568 (1985).

[7] P. J. Dean, J. R. Haynes, and W. F. Flood, Phys. Rev. **161**, 711 (1976).

[8] B. L. Gel'mont, N. N. Zinov'ev, D. I. Kovalev et al., Zh. Eksp. Teor. Fiz. **94**, 322 (1988) [Sov. Phys. JETP **67**, 613 (1988)].

[9] N. N. Zinov'ev, D. I. Kovalev, I. D. Yaroshetskiĭ, and A. Yu. Blank, Pis'ma Zh. Eksp. Teor. Fiz. **53**, 147 (1991) [JETP Lett. **53**, 154 (1991)].

[10] P. Norton, Phys. Rev. Lett. **37**, 164 (1976).

[11] V. N. Aleksandrov, E. M. Gershenzon, A. P. Mel'nikov et al., Pis'ma Zh. Eksp. Teor. Fiz. **22**, 573 (1975) [JETP Lett. **22**, 282 (1975)].

[12] W. Burger and K. Lassmann, Phys. Rev. Lett. **53**, 2035 (1984).

Translated by M. E. Alferieff